Cell Organoid

Article

https://doi.org/10.26599/CO.2024.9410001

Patient-derived skin tumor organoids with immune cells respond to metformin

Authors

Yanghua Shi, Jiping Liu, Lanyang Li, Chen Wang, Jian Zhang, ..., Jun Chen*, Chunhui Cai*, Xinxin Han*

Correspondence

Jun Chen, chenjun125125@126.com; Chunhui Cai, caichunhui@lishengbiotehc.com; Xinxin Han, xxhan@sibs.ac.cn

In Brief

Here, we developed patient-derived skin tumor organoids mimicking clinical tissues, showcasing diverse cell types and immune interactions. Single-cell sequencing identified 11 cell types, highlighting fidelity to in vivo counterparts. Bermatofibrosarcoma protuberans (DFSP) organoids revealed metformin's unique immune signaling modulation, aiding drug testing and mechanistic exploration.

Graphical abstract

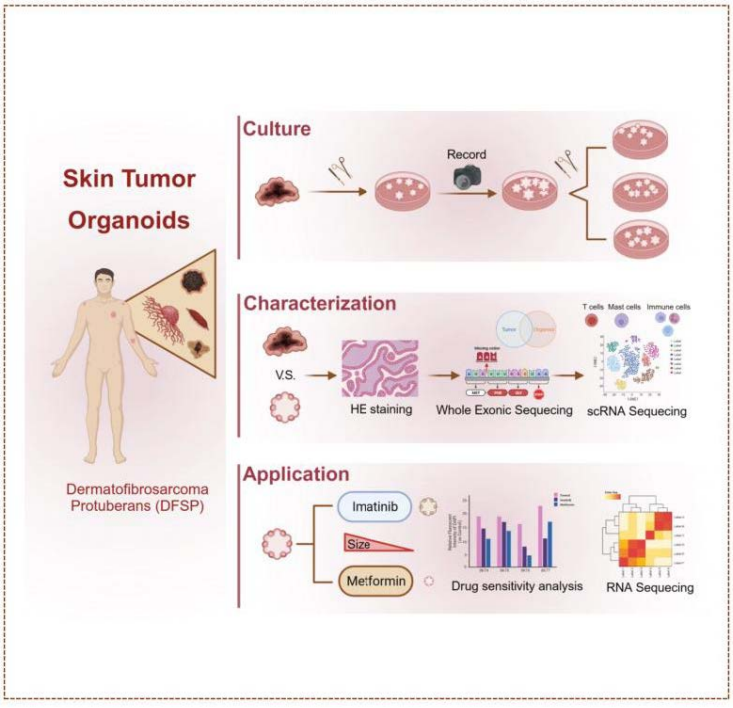

Highlights

- Patient-derived skin tumor organoids replicate clinical tissue characteristic
- Single-cell sequencing identifies 11 distinct cell types in skin organoids
- Bermatofibrosarcoma protuberans (DFSP) organoids used to test responses to imatinib and metformin
- Metformin inhibits the growth of DFSP organoids via immune signaling pathway

Cell Organoid

Article

https://doi.org/10.26599/CO.2024.9410001

Patient-derived skin tumor organoids with immune cells respond to metformin

Yanghua Shi[1,§], Jiping Liu[1,§], Lanyang Li[1], Chen Wang[1], Jian Zhang[1], Mingjie Rong[1], Yamin Rao[2], Xiaobo Zhou[3], Di Sun[4], Jun Chen[3,*], Chunhui Cai[1,*], and Xinxin Han[1,5,*]

[1] *Shanghai Lisheng Biotech, Shanghai 200092, China*
[2] *Department of Pathology, Shanghai Ninth People's Hospital, affiliated to Shanghai Jiao Tong University School of Medicine, Shanghai 200011, China*
[3] *Department of Dermatology and Dermatologic Surgery, Shanghai Ninth People's Hospital, affiliated to Shanghai Jiao Tong University School of Medicine, Shanghai 200011, China*
[4] *Department of Plastic and Reconstructive Surgery, Shanghai Ninth People's Hospital, affiliated to Shanghai Jiao Tong University School of Medicine, Shanghai 200011, China*
[5] *Organ Regeneration X Lab, LiSheng East China Institute of Biotechnology, Peking University, Nantong 226299, China*
[§] *Yanghua Shi and Jiping Liu contributed equally to this work.*

Received: 23 January 2024 / **Revised:** 26 March 2024 / **Accepted:** 6 April 2024

ABSTRACT

Surgery is the primary treatment for skin tumors, but it can result in scarring and distress for patients. Developing alternative therapeutic methods necessitates suitable *in vitro* models, which are currently limited in accurately representing the *in vivo* cell types and microenvironment of skin tumors. Here, we present a practical approach for creating patient-derived skin tumor organoids that effectively replicate the histological characteristics and mutational profiles observed in clinical tissues. Utilizing single-cell sequencing, we identified up to 11 distinct cell types within the organoid samples, encompassing various skin system cells and immune cells. Furthermore, we demonstrate the applicability of bermatofibrosarcoma protuberans (DFSP) organoids for assessing their responses to imatinib and metformin. Our findings reveal that metformin, in contrast to imatinib, can modulate the expression of downstream genes through immune signaling pathways. Our results underscore the ability of DFSP organoids to preserve key features of clinical tissues, including the presence of multiple cell types, especially immune cells. Importantly, our organoids provide a convenient approach for investigating the effects of drugs and elucidating underlying molecular mechanisms.

KEYWORDS

skin tumor, keloid, dermatofibrosarcoma protuberans (DFSP), patient-derived organoid (PDO), drug screening, immune cells therapy, metformin, imatinib

Introduction

Surgical intervention remains the primary treatment for skin tumors, despite its potential to result in scarring and patient distress. The development of alternative therapeutic methods necessitates suitable *in vitro* models, which are currently limited in accurately representing the *in vivo* cell types and microenvironment of skin tumors. The skin serves as a crucial barrier between the body and the external environment, playing a pivotal role in protecting against pathogens and environmental insults[1–3]. The intricate network of immune cells residing in the skin, plays a central role in maintaining skin homeostasis and defending against pathogens[4–6]. In addition to their role in protection, immune cells in the skin are also involved in the pathogenesis of various skin diseases, contributing to both inflammatory and autoimmune conditions[7–9]. The establishment of a useful *in vitro* skin tumor model incorporating original immune cells may provide insights into the complex interplay between the skin and the immune system, unraveling the mechanisms underlying skin tumors, and facilitating the development of effective therapeutic strategies.

Dermatofibrosarcoma protuberans (DFSP) is an uncommon cutaneous sarcoma with a high local recurrence rate, low metastatic rate, and low mortality, and its incidence has remained stable over the years[10]. Both Mohs surgery and wide local excision (WLE) are viable surgical options for treating DFSP. Mohs surgery may minimize reconstruction needs due to smaller

*Address correspondence to Jun Chen, chenjun125125@126.com; Chunhui Cai, caichunhui@lishengbiotehc.com; Xinxin Han, xxhan@sibs.ac.cn

Cite this article as Shi, Y. H., et al. *Cell Organoid*, **2024**, 1: 9410001.

average defect sizes and may result in fewer complications, but may also result in asymmetry. Immediate flap reconstruction, especially in larger defects, can achieve aesthetic results for DFSP patients without compromising the detection of disease recurrence[11–13]. Given the high recurrence rate of DFSP and its low mortality, the development of alternative treatment modalities, such as systemic (oral) or localized (topical) pharmacotherapy, is of paramount importance to enhance clinical outcomes. However, the research on in vitro models for DFSP is still insufficient[14]. Recently, some novel patient-derived models have been established. Two cell lines, NCC-DFSP1-C1 and NCC-DFSP2-C1, were derived from two patients with DFSP. These cell lines preserved the unique collagen type I alpha 1 chain (COL1A1) -PDGFB translocation characteristic of DFSP, which causes constitutive activation of the platelet-derived growth factor β (PDGFB) signaling pathway. In vitro screening studies identified anticancer drugs that showed antiproliferative effects at considerably low concentrations in the DFSP cell lines. These cell lines could be used for developing novel therapeutic strategies to treat DFSP[15]. Although some progress has been made, there is still an urgent need to develop an *in vitro* three-dimensional (3D) model for DFSP including the immune microenvironment in order to better understand the biology of this disease and develop effective treatment methods.

In the field of cancer research, organoids, also known as tumoroids, serve as an important component for the discovery of potential therapeutic targets and the identification of novel compounds[16]. They have been shown to more accurately recapitulate the structures, specific functions, molecular characteristics, genomic alterations, expression profiles, and tumor microenvironment of primary tumors [17]. Patient-derived organoids (PDOs) have been used as a tool for personalized medical decisions to predict patients' responses to therapeutic regimens and potentially improve treatment outcomes[18]. In skin tumor study, researchers used hydrogel-based engineering techniques to develop patient-specific sarcoma organoids, including DFSP[19]. The organoids were screened for chemotherapy efficacy, and a subset was enriched with a patient-matched immune system for screening of immunotherapy efficacy. The study concluded that a large subset of sarcoma organoids does not respond to chemotherapy or immunotherapy, as seen in clinical practice[19]. Specifically, skin organoids can not only highly simulate the physiological structure and function of skin tissue, better restore the real skin ecology under different *in vitro* environments, but also be applied to skin development research, skin disease pathology research and drug screening and other fields[20,21].

Imatinib, a tyrosine kinase inhibitor, has been identified as a safe and effective treatment for DFSP[22]. It has shown significant efficacy in advanced cases of DFSP, reducing tumor size preoperatively and lessening surgical morbidity associated with the removal of residual DFSP[23]. The drug works by targeting the COL1A1-PDGFB fusion gene, a result of the distinctive rearrangement of chromosomes 17 and 22 that underlies the development of DFSP[24]. However, the use of imatinib as a neoadjuvant therapy, aimed at reducing tumor size for complex surgical cases, requires careful patient selection and consideration of potential risks and benefits, especially when the tumor is in a cosmetically or functionally significant area or when incomplete excision could lead to high local risk. Despite imatinib's general tolerability and favorable therapeutic index, the pharmacological benefits and toxicity risks for each patient must be evaluated[23].

In our study, we present a rapid method for the generation of skin tumor organoids without the use of enzymes or Matrigel. Our organoids exhibited proliferative capacity across multiple generations, reaching a substantial volume comparable to 2 mm^3. Histological and genomic analyses revealed the resemblance between the organoids and clinical tissues. Single-cell sequencing data identified 11 distinct cell types within the skin tumor organoids, encompassing immune cells and various skin cell types. RNA sequencing of four distinct DFSP organoids further confirmed the diverse cell populations within our cultured organoids. Additionally, we evaluated the responsiveness of our organoids to imatinib and metformin, both of which effectively inhibited the growth of DFSP organoids. Notably, metformin was found to modulate the expression of immune signaling pathways. Collectively, these findings underscore the potential utility of our patient-derived skin tumor organoids for drug testing and mechanistic studies.

Results

Culture of skin tumor organoids from patient tumors without enzymatic dissociation

In order to maintain the native micro-environment of tumor tissues, and to decrease the risk of clonal selection of specific cell populations, we developed a method to generate skin tumor organoids without enzymatic dissociation of tumor tissues into single cells (Fig. 1a). Furthermore, we did not use Matrigel or other biomaterials to support organoid growth, the skin tumor organoids were cultured either suspend or adherent or both in the culture medium. Freshly resected skin tumor tissue was collected from patients after surgery with full informed consent (Fig. S1(a) in the Electronic Supplementary Material (ESM)). The tissue samples were soaked in a washing solution for 3 minutes and then transferred to a 50 mL centrifuge tube for three rounds of washing. After decanting the excess liquid, the tissue blocks were placed in a 10 cm culture dish, and 100–200 μL of culture medium was added. The tissue blocks were then cut into approximately 0.5–1 mm^3 microtissue blocks and transferred to a new 10 cm culture dish, with 1 mL of culture medium added to resuspend the microtissue blocks. Finally, 15 mL of culture medium was added to maintain the organoid culture (Fig. 1a). Image records were taken for each skin tumor organoid to observe morphological differences among patients. A total of 10 tumor samples detected on skin were collected after surgery from the center part of lesion area, including 2 keloid patients, 1 melanoma patient, 1 malignant schwannoma patient, and 6 DFSP patients (Figs. S1(a) and S1(b) in the ESM). Due to the rarity of DFSP, a skin cancer with no reliable *in vitro* study method, we focused on the culture and characterization of DFSP organoids in our subsequent study.

To evaluate the growth characteristics of organoids from different patients, images were captured at various time points (Fig. 1b and Fig. S1(c) in the ESM). Once the organoid volume reached 2 mm^3 or the margin became smooth, we sub-cultured large organoids into smaller ones using a mechanical dissociation method (Fig. 1a). Quantitative analysis of organoid volumes using ImageJ revealed proliferative capacity in both P0 and P1 (Fig. 1c).

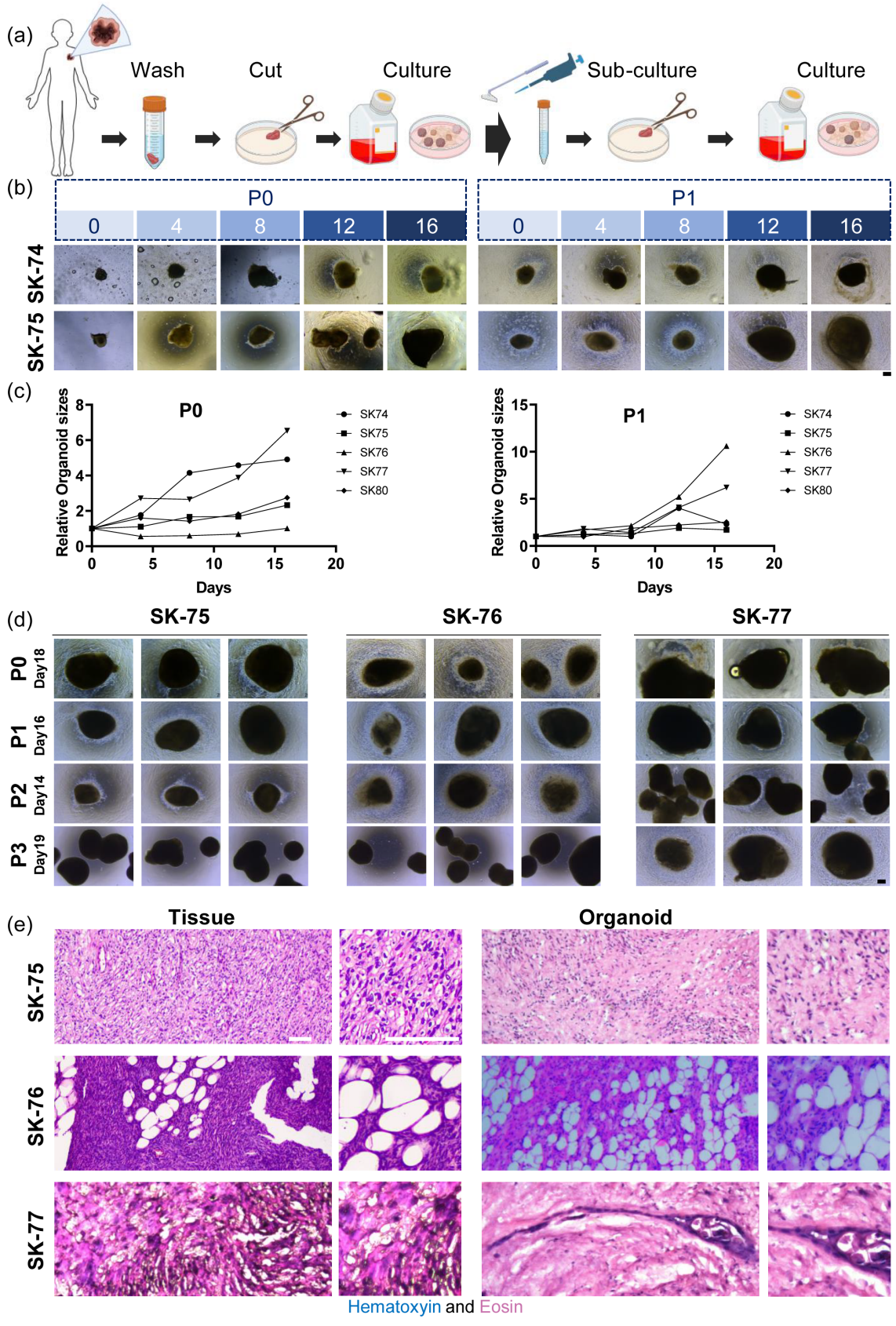

Figure 1. Culture and characterization of skin tumor organoids. (a) Schematic diagram of organoid culture and passaging process. (b) Growth records of organoids from different patients, with organoids at P0 on the left and at P1 on the right; scale bar = 200 μm. (c) Statistical chart of organoid growth volume at different generations. (d) Bright-field images of DFSP organoids at different generations from P0 to P3; scale bar = 200 μm. (e) Comparative histological images of clinical tissue and organoids stained with H&E staining; scale bar = 50 μm.

The growth curves for SK75 and SK80 organoids were similar in both generations; however, for SK74 and SK77 organoids, the P0 generation exhibited higher cell growth ability than P1. Conversely, for SK76 organoids, the P0 generation showed lower cell growth ability than P1. Our observations indicated that the growth speed and maximum volume of cultured organoids did not correlate with different generations (Fig. 1d).

To determine whether DFSP organoids resemble their clinical tumor tissues, we conducted histological examinations. Hematoxylin and eosin (H&E) staining revealed cellular types and distribution within the DFSP organoids that closely resembled those found in clinical tissues (Fig. 1e). Additionally, we observed morphological inter-patient heterogeneity. DFSP organoids exhibited spindle-shaped cancer cells (SK75), multiple adipocytes (SK76), and disordered cells (SK77).

Characterization of genetic mutations between DFSP organoids and tissues

To assess whether DFSP organoids maintain genomic alterations of tumor tissues, we performed whole exome sequencing (WES) of three pairs of samples (SK74/SK75/SK77) from different patients (Fig. 2a). The number and locations of genetic mutations in the exons between their clinical tissues and organoids were analyzed. The WES results showed around 80% concordance rate of mutation sites between the clinical tissues and organoid samples from the same patient (Fig. 2b). The organoids of patients SK74 and SK77 exhibited more mutation sites (Fig. 2a). Subsequently, we performed an overlap analysis of mutation sites from the three different patients (Fig. 2c), and the data showed that the complete overlap of mutation sites among the three patients compared to their respective mutation site numbers was not very high, being less than 40% (Fig. 2d). This result reflects the sample heterogeneity among different patients and reveals the complexity of the disease. According to a literature reference describing DFSP gene alterations[25], we extracted the highly frequent mutation sites in this disease to create a heatmap and found that the three patients selected in our study all conformed to the conclusions mentioned in the published article, and maintained a high degree of consistency between the organoids and tissues (Fig. 2e). Finally, we also conducted an in-depth analysis of our own WES data to identify some specific gene mutation sites, which included both SNPs (Fig. 2f) and Indels (Fig. 2g). These mutation proportions were consistent between the tissues and organoids of the same patient, but were significantly different among samples from different patients. For example, the SNP of *PRSS3* was only found in SK74 and SK75, while SK77 had a higher proportion of Indel mutations in *PRSS3* (Figs. 2f and 2g).

Single-cell sequencing data reveals immune cells within the skin tumor organoids

In order to explore the cellular microenvironment and molecular characteristics of distinct skin tumors, we conducted single-cell sequencing on keloid and DFSP organoids. Given the similar appearance of keloid and DFSP patients, which can lead to misdiagnosis, it was crucial to discern the molecular variances between them. Organoids were collected from two patients for each disease once the cultured organoid size reached 2 mm^3. By comparing our single-cell data from the four organoid samples with publicly available single-cell sequencing data from skin samples, we were able to identify up to 11 different cell types in our organoid samples (Fig. 3a)[26]. These cell types encompassed common skin system cell types such as endothelia, fibroblast, glandular, keratinocyte, melanocytes, and muscle fiber, as well as immune cells like lymphatic endothelia, mast cells, and T cells. Examination of the single-cell data from the four organoid samples individually revealed an abundance of fibroblast cells in the DFSP organoids, while immune-related cells were relatively scarce. Conversely, the keloid organoids displayed a higher presence of keratinocyte and T cells, indicating diverse immune microenvironments in cultured organoids from different diseases (Fig. 3b). Furthermore, weighted gene co-expression network analysis (WGCNA) of gene expression in keloid and DFSP organoids demonstrated unique gene expression characteristics for each patient (Figs. S2a and S2b in the ESM).

Cell-type heterogeneity and molecular signatures by DFSP organoids

To further investigate cell-type heterogeneity in DFSP organoids, we conducted RNA-seq analysis on four distinct sets of organoids once the cultured organoid size reached 2 mm^3 in their P0 generation, including SK74, SK75, SK76 and SK77 (Fig. S1b in the ESM). Each organoid underwent two independent experimental replicates, with the second experiment including two parallel controls, resulting in three datasets for each organoid. The clustering analysis of the RNA-seq data was consistent with our sample collection (Fig. 3d). Both principal component analysis (PCA) and gene clustering analysis revealed substantial heterogeneity among the four organoids (Figs. 3e and 3f). Upon annotating the RNA-seq data with network information, the distribution of different cell types in the four organoids was visually discernible (Fig. 3g). For SK74 and SK75, cell-types distribution results by RNA-seq analysis were similar as the single cell sequencing results. Notably, the SK77 organoid, collected at 20 days, emerged as the youngest among the group, exhibited a comparatively higher proportion of each cell type, whereas the remaining three organoids displayed distinct dominant cell populations (Fig. 3g). Subsequent WGCNA partitioned the differentially expressed genes of the four organoids into eight distinct modules (Fig. S2c in the ESM). The gene expression profiles also demonstrated marked disparities between SK77 and the other samples. KEGG/GO analysis unveiled the upregulated signaling pathways in each module (Fig. S2d in the ESM), with the turquoise module specifically upregulated in the SK77 sample. Notably, the Defense response to virus and Angiogenesis pathways were significantly upregulated. A comprehensive investigation of key genes in these pathways may yield potential therapeutic targets in the future. This heterogeneity may stem from inter-individual variations among patients or differences in organoids validation time points[17,27–29].

Imatinib and metformin effectively inhibit the growth of DFSP organoids

To assess the suitability of DFSP organoids for drug sensitivity screening and drug discovery, we conducted experiments using the clinically approved drug Imatinib and the potential anti-cancer drug metformin. Metformin has been repurposed for several emerging applications, including as an anti-cancer agent[30]. It has been found to have anti-cancer effects and is associated with reduced risk of cancer and decreased cancer-related mortality in patients with diabetes[31]. Treatment of the organoids individually

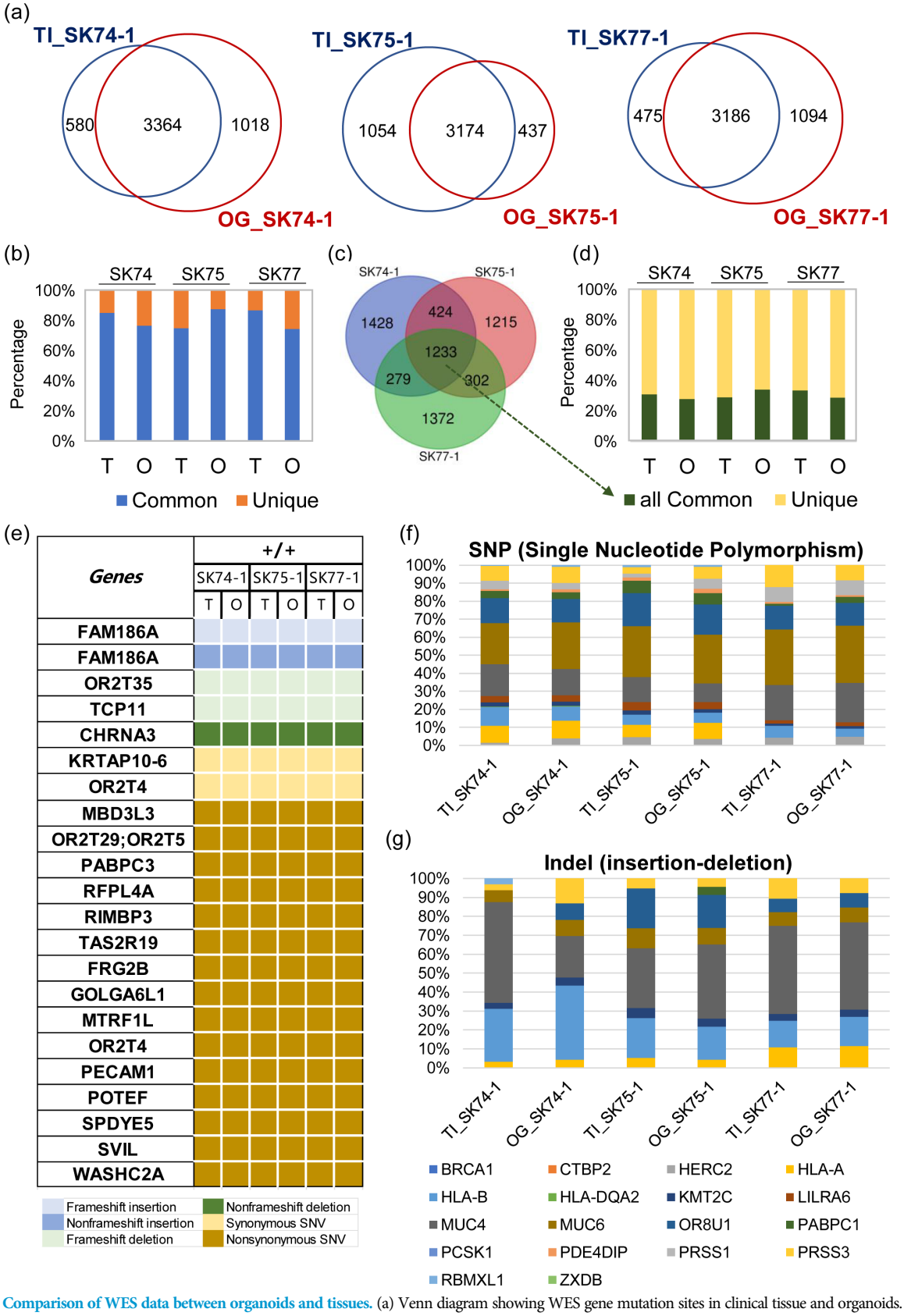

Figure 2. Comparison of WES data between organoids and tissues. (a) Venn diagram showing WES gene mutation sites in clinical tissue and organoids. (b) High consistency between clinical tissue and organoids from the same patient, with an overlap rate close to 80% (n = 3, SK74/SK75/SK77). (c) Venn diagram of WES gene mutation sites from three different patients. (d) Low overlap rate of WES mutation sites among three different patients, less than 40%, demonstrating patient heterogeneity. (e) Consistency between clinical tissue and organoid samples was observed, as reported by Peng et al. in their study on genomic alterations of dermatofibrosarcoma protuberans. (f) WES data analysis revealed different mutation sites of certain genes among different patients.

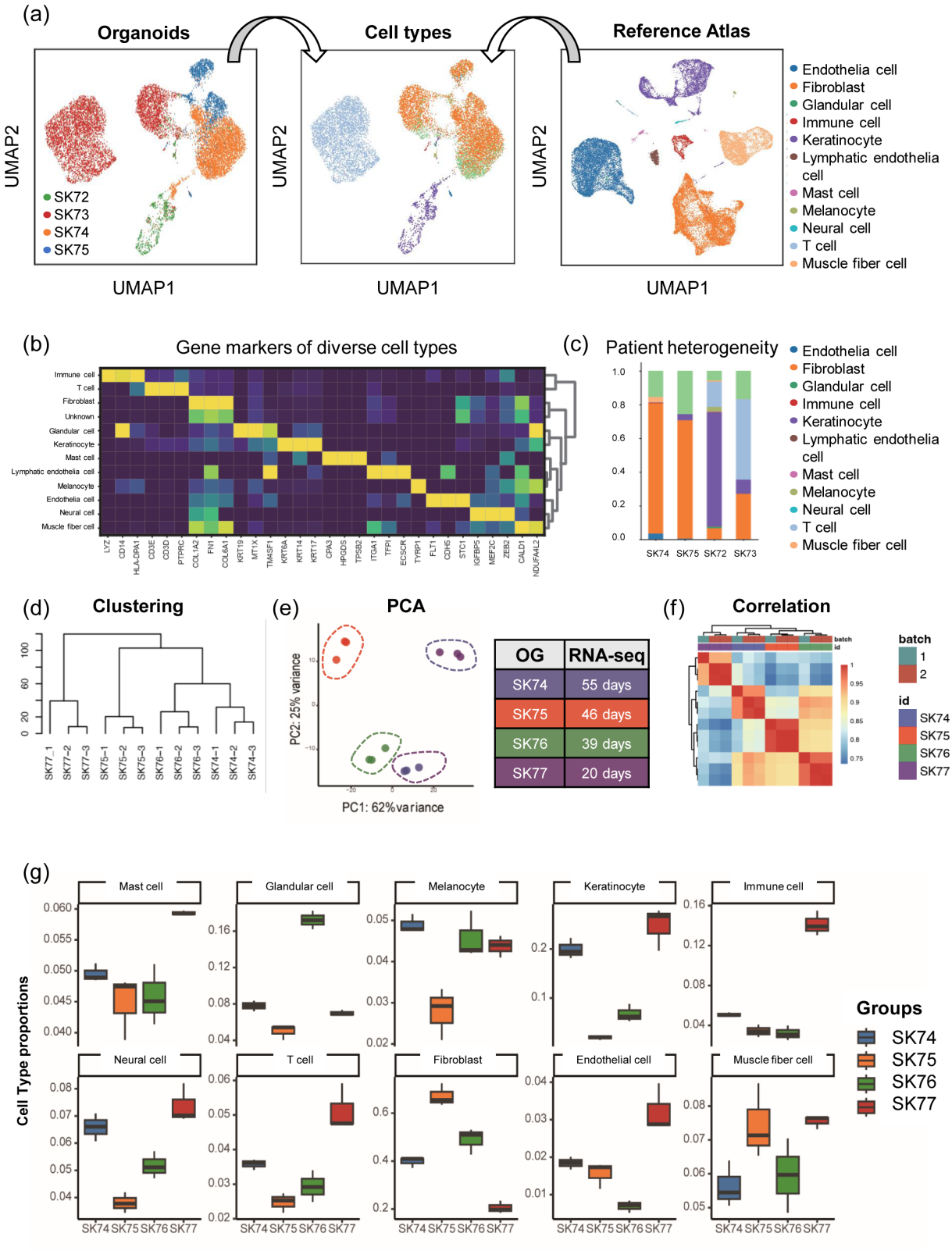

Figure 3. Diverse cell types in the cultured skin organoids. (a) Cell type definition based on comparison with public network data. (b) Identification of marker genes for different cell types. (c) Variation in cell type composition and proportions across the four organoids. (d) Three replicates of each of the four organ types were clustered and collected at different time points. (e) RNA-seq data was analyzed using PCA. (f) Gene clustering analysis was performed on the four organoids. (g) The proportions of different cell types varied across the four organ types.

with Imatinib (SK74/SK75/SK76) revealed significant inhibition of organoid sphere enlargement in SK74/SK75 compared to the control group (Fig. 4a). Notably, distinct phenotypic variations were observed under drug inhibition, with SK74 exhibiting rapid

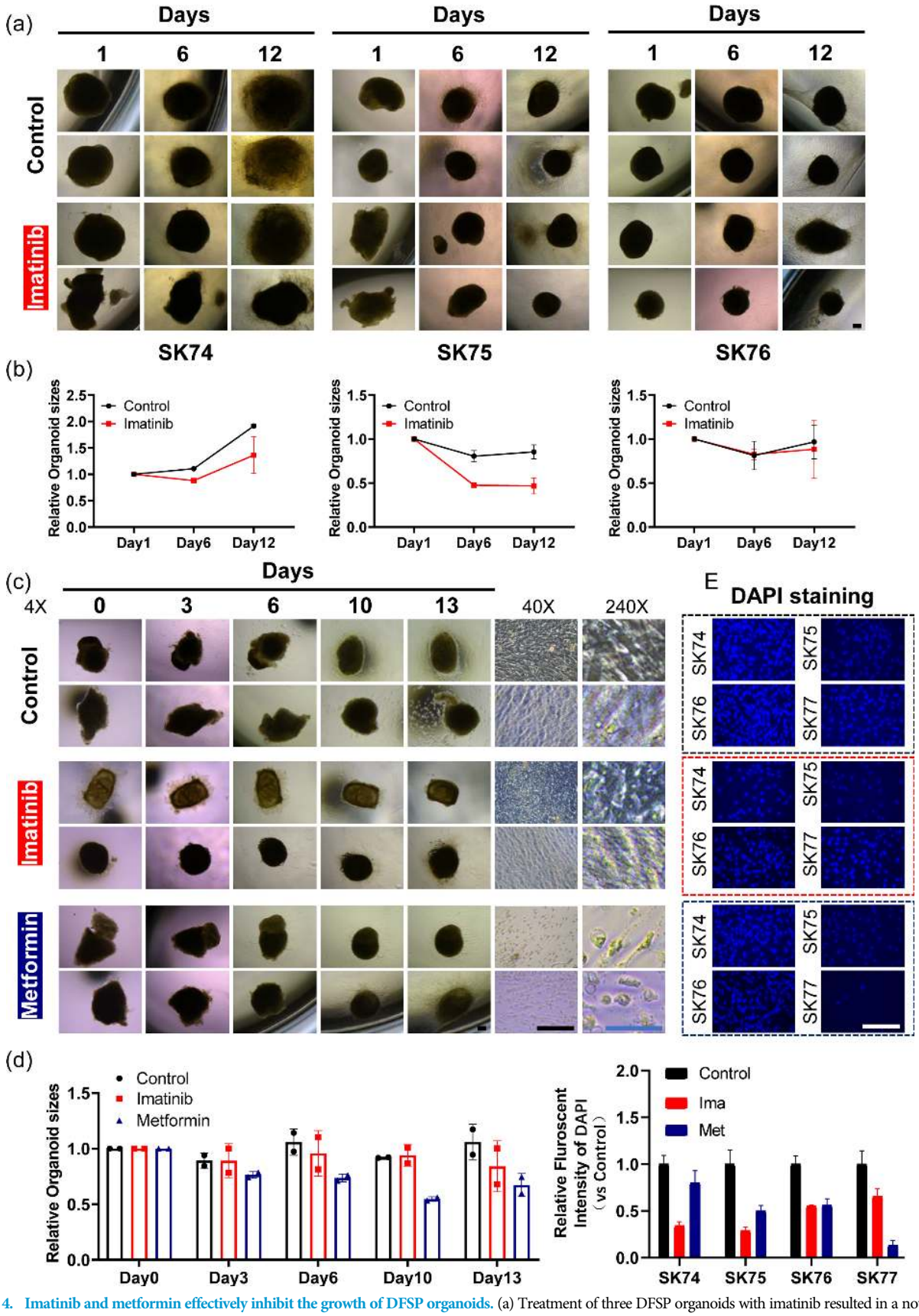

Figure 4. Imatinib and metformin effectively inhibit the growth of DFSP organoids. (a) Treatment of three DFSP organoids with imatinib resulted in a noticeable reduction in organoid sphere volume in two organoids, SK74 and SK75, with no significant effect observed in SK76; scale bar = 200 μm. (b) Statistical line graph depicting organoid volume sizes. (c) Record of organoid growth after treatment with imatinib and metformin, showing a significant decrease in the number of adherent cells in the drug-treated groups on the thirteenth day; black scale bar = 200 μm; blue scale bar = 50 μm. (d) Statistical bar graph representing organoid volume sizes. (e) Bar graph showing the number of adherent cells counted after DAPI staining; scale bar = 200 μm.

organoid sphere volume increase and edge-differentiated cell morphology in the control group. In contrast, SK75 organoid spheres became more compact with no significant volume increase, and imatinib led to the appearance of smaller organoid spheres (Fig. 4b). Furthermore, treatment of the SK77 organoids with the previously untested drug metformin resulted in effective inhibition of organoid sphere volume from the sixth day to the thirteenth day. This was accompanied by a significant decrease in cell numbers, along with notable changes in cell morphology and size (Figs. 4c and 4d). Subsequent testing on additional organoids confirmed the therapeutic efficacy of both drugs after 13 days of treatment, as evidenced by DAPI staining data of the adherent cells (Fig. 4e). These drug experiments provided compelling evidence that DFSP organoids can serve as a valuable method for drug sensitivity testing and new drug screening.

Metformin inhibited DFSP organoids via immune related pathways

Based on the pronounced phenotypic responses of DFSP organoids to imatinib and metformin, we sought to further elucidate the molecular mechanisms underpinning the pharmacological actions of these agents. To this end, we performed RNA-seq analysis on collected samples. Following a similar experimental design to previous studies, we selected four organoids (SK74, SK75, SK76, and SK77) and conducted two independent experiments, with the second experiment involving two sets of parallel samples, resulting in three replicates for each treatment condition. Principal component analysis (PCA) revealed a higher degree of sample consistency compared to the drug treatment results (Fig. 5a), while gene expression clustering analysis further confirmed inter-sample heterogeneity (Fig. 5b). Subsequent Weighted gene co-expression network analysis (WGCNA) aimed to identify shared changes following drug treatment, disregarding inter-organoid heterogeneity. We categorized downstream pathway changes into six distinct modules, and the results indicated that Imatinib treatment exhibited closer resemblance to the control group, whereas metformin treatment led to relatively substantial alterations in gene expression compared to the control and Imatinib treatment groups (Fig. 5c). Following metformin treatment, three modules (yellow, blue, and green) exhibited marked upregulation, with KEGG/GO analysis revealing enrichment of pathways related to cell cycle, phagocytosis, B cell activation, P53 signaling, immune system development, and ERK1/ERK2 cascade (Fig. 5d). Concurrently, three modules (red, turquoise, and brown) displayed significant downregulation following metformin treatment, with KEGG/GO analysis indicating pronounced downregulation of genes associated with pathways such as DNA transcription, apoptotic pathway, Innate-immune response, Wnt signaling, T cell differentiation, DNA replication, and TOR signaling (Fig. 5e). We suggested that the upregulated immune system development and downregulated innate-immune response after metformin treatment may be a response by the immune cells maintained in our cultured organoids (Figs. 3c and 3g).

Discussion

In contrast to previously reported tumor organoids derived from dissociated tumor cells, devoid of red blood cells, our skin tumor organoids maintain the native cell microenvironment and original tissue structure. Unlike the complex procedures involving Matrigel for organoid establishment, our culture system requires only 30 min to 1 h, based on a robust culture medium and mechanical dissociation. The skin tumor organoids demonstrate consistency with clinical tissues, as evidenced by histological analyses revealing similar tissue architecture and cellular morphologies, whole-exome sequencing confirming the preservation of somatic variants at comparable frequencies, and single-cell sequencing revealing the maintenance of multiple cell populations. Furthermore, heterogeneity between patients is evident, as observed through single-cell RNA-seq, which identifies different dominant cell types, and RNA-seq, which demonstrates diverse cell distributions in DFSP organoids. Additionally, we employed DFSP organoids to investigate the functional effects and genetic mechanisms of imatinib and metformin. Imatinib, a U.S. Food & Drug Administration (FDA)-approved drug, acts as an antagonist to inhibit tyrosine kinase, effectively suppressing the growth of DFSP organoids without modulating the expression of other genes. Conversely, metformin depresses the proliferation of DFSP organoids by modulating immune signaling pathways. Our practical and rapid method for culturing skin tumor organoids holds promise for advancing disease drug development.

The generation of traditional cancer organoid models typically involves the use of enzymatic digestion to dissociate clinical tissues into single cells, followed by the formation of 3D spheres with the aid of Matrigel or other biomaterials, resembling the primary culture method[17]. However, recent studies have proposed the establishment of tumor organoids using mechanical methods to preserve the optimal tumor microenvironment and cell–cell interactions by separating clinical tissues into small pieces without enzymatic treatment[32–35]. For instance, the glioma organoid (GBO) initiative has successfully created a live biobank of GBOs from 53 patients with diverse mutational profiles, serving as a valuable resource for future biological studies and therapeutic testing[32]. Given the rarity of DFSP, sample collection poses a significant challenge. In our study, we utilized samples from 10 skin tumor patients, including 6 DFSP patients. The limited number of available samples underscores the need to establish a larger biobank and information repository to comprehensively capture underlying patterns. This approach is crucial for advancing our understanding of DFSP and facilitating future research and therapeutic development.

When establishing a disease organoid model, it is essential to consider the tissue's spatiotemporal specificity. Several studies have highlighted the spatiotemporal specificity of cancer tissue. For example, the Marco group has utilized bulk and single-cell genomic approaches to characterize genetic and transcriptional heterogeneity in glioblastoma (GBM), patient-derived explants (PDEs), and gliomasphere (GS) lines[33]. Given the distinct distribution of DFSP tumor tissue, the generation of singular tumor-specific organoids from the central part of the tumor is insufficient for accurately depicting the complete landscape of disease initiation and recurrence. There is a critical need for more sophisticated organ models to comprehensively investigate tumor regions and their surrounding areas. This approach is essential for gaining a deeper understanding of disease progression and developing more effective therapeutic strategies.

It is evident that organoids present challenges in terms of culture periods and consistency maintenance as comparing to two-dimensional (2D) primary culture methods and mouse models. However, organoids can better mimic the cellular microenvironment of tissues compared to 2D cell culture systems, and they more accurately represent tissue physiology[36]. They

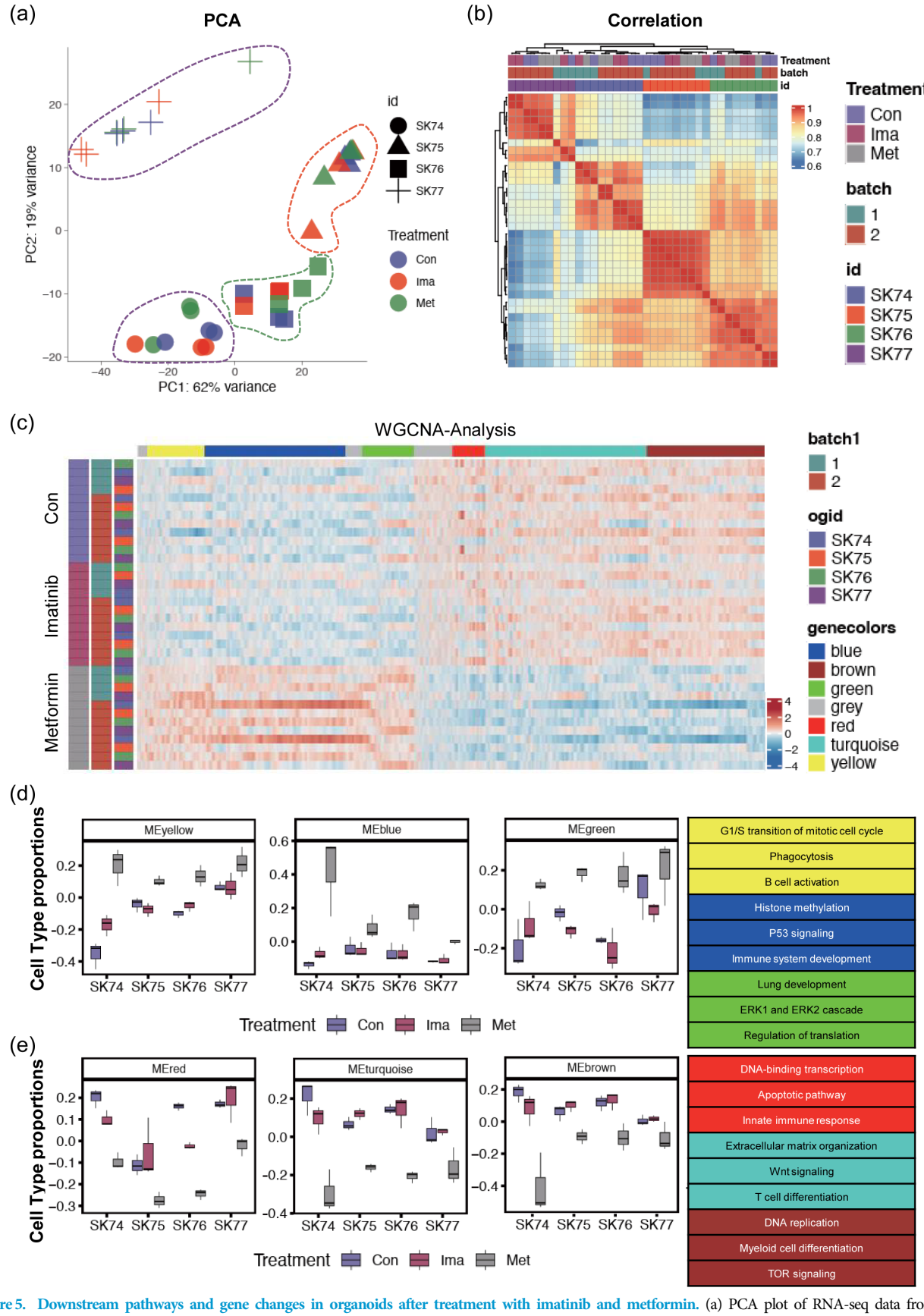

Figure 5. Downstream pathways and gene changes in organoids after treatment with imatinib and metformin. (a) PCA plot of RNA-seq data from four organoid samples after drug treatment. (b) Clustering plot of gene expression in three replicates of the four organoid samples. (c) WGCNA analysis conducted to identify gene expression differences among the four organ types after treatment with the two drugs. (d) Display of relevant signaling pathways within three upregulated modules after metformin treatment. (e) Display of relevant signaling pathways within three downregulated modules after metformin treatment.

exhibit higher cellular heterogeneity, organization, and tissue-like structures, making them a more relevant *in vitro* model for functional analyses and personalized therapies[37]. On the other hand, mouse models, being the closest to recapitulating human tissue functions and cellular interactions, can predict the development of treatments or diseases. However, they are limited by differences in species biology, sensitivity variations, high maintenance costs, and limited throughput. In contrast, 2D monolayer cell cultures, while more basic than animal models, provide insight into complex diseases with low cost, time efficiency, and high reproducibility. Nevertheless, they fail to recapitulate the complexity of the *in vivo* microenvironment due to the absence of an extracellular matrix (ECM), hindering the natural development of cells and tissues[38]. However, the choice of model often depends on the specific research question being addressed. Additionally, these models can be used complementarily in various research scenarios. In our study, we conducted single-cell RNA sequencing and bulk RNA sequencing when the cultured organoids reached a threshold volume of 2mm^3, which determined whether they would be subcultured to the next generation. Notably, each organoid reached this standard at different time points. However, based on our unpublished data, the differences in culture times within the same generation of organoids may not lead to genetic differences.

The single-cell sequencing results shown the skin tumor organoids have 11 distinct cell types including immune cells which indicating the possibility to use this culture method to test the drugs of immune therapy. Metformin, a common drug used for diabetes, has been found to have multiple anti-cancer effects. It can downregulate ACSL4 expression in early stages of colorectal cancer[39], improve the fitness of CD8 T cells in hypoxic conditions[40], and inhibit the Wnt signaling pathway, which is involved in cell proliferation and survival[41]. Further, metformin activates AMPK, enhances the anti-cancer activity of γδ T cells, providing a potential new approach for cancer immunotherapy[42]. Our RNA-seq analysis of DFSP organoids treated with metformin confirmed these genetic modulations. KEGG analysis indicated that metformin could inhibit the growth of DFSP organoids through immune signaling pathways. This suggests the potential for metformin to be repurposed as a therapeutic agent for DFSP, particularly in the context of immune modulation.

Based on the above experimental results, we believe that organoids have potential in the field of research and treatment of DFSP. Detailed genotyping is indeed crucial for the selection of drugs in personalized treatment. It allows for a better understanding of the genetic makeup of an individual's disease, which can guide the choice of therapeutic strategies. When combined with WES and RNA-seq data, it can help identify population heterogeneity, which is key to understanding the diverse responses to treatment observed among patients. Organoid databases and samples offer numerous advantages in the context of drug testing. They mimic the cellular microenvironment of tissues better than 2D cell culture systems and represent the tissue physiology. This makes them more physiologically relevant, providing a more accurate model for drug testing. Organoids capture the cellular composition and pharmaco-typic signatures of the parental tumor. This allows for a better understanding of how drugs might interact with different cell types within a tumor. Organoids have been applied in drug screening to demonstrate the correlation between genetic mutations and sensitivity to targeted therapy. This can help predict how a patient's tumor might respond to a particular drug. PDOs can provide clinicians with a model system to choose the most effective treatment options for individual patients. This is a significant step towards personalized medicine. Organoids offer reproducibility, which is crucial in drug testing. Biobanks can be generated for repeat study. Organoids hold great promise for toxicological drug and compound screening and could potentially reduce the use of non-human animals for the same purpose. Experiments on the effects of imatinib and metformin on DFSP organoids provide valuable information. Treatment of the organoids individually with Imatinib revealed inhibition of organoid sphere enlargement in SK74/SK75 compared to the control group. Notably, distinct phenotypic variations were observed under drug inhibition. Treatment of the SK77 organoids with Metformin resulted in effective inhibition of organoid sphere volume from the sixth day to the thirteenth day. This was accompanied by a decrease in cell numbers, along with notable changes in cell morphology and size. Subsequent testing on additional organoids confirmed the therapeutic efficacy of both drugs after 13 days of treatment, as evidenced by DAPI staining data of the adherent cells. These findings suggest that DFSP organoids can serve as a valuable method for drug sensitivity testing and new drug screening.

Methods and materials

Tissue collection

The clinical tissue sample collection methodology adhered to strict ethical guidelines and standard operating procedures to ensure the integrity and quality of the collected samples. Key steps in the methodology included patient identification, informed consent, sample collection, processing, storage, and documentation. The collection of clinical tissue samples was conducted by trained medical personnel, following established protocols to minimize contamination and ensure the preservation of sample viability for downstream analysis. Additionally, stringent record-keeping and labeling practices were implemented to maintain traceability and facilitate accurate data management. All the clinical samples were collected under the Shanghai Ninth People's Hospital ethical guidelines and were assigned the ethical code 2017125.T321.

Organoid culture

The tissue specimens were soaked in a washing solution (LSNO00100201; Shanghai LiSheng Biotech, China) for 3 min and then transferred to a 50 mL centrifuge tube for 3 rounds of washing using washing solution. Each wash involved the addition of 5 mL of washing solution and gentle agitation to cleanse the tissue surface. After decanting the supernatant, the tissue blocks were transferred to a 10 cm culture dish, where 100–200 μL of culture medium (LSTO015004; Shanghai LiSheng Biotech, China) was added. The tissue blocks were then cut into approximately 1 mm^3 microtissue blocks and transferred to a new 50 mL tube. Following the addition of 1 mL of culture medium to resuspend the microtissue blocks, they were transferred to a new 10 cm culture dish. The remaining tissue was collected and transferred to a new dish after rinsing with 1 mL of culture medium. Finally, 15 mL of culture medium were added to maintain the organoids

culture.

During the organoid culture process, a partial medium change should be performed every 5–7 days, or as needed based on changes in the color and turbidity of the medium, to ensure an adequate supply of nutrients for organoid growth. The specific steps for partial medium change involve opening the top cover of the culture container, tilting the container to allow the organoids to settle, and then using a 1 mL regular pipette tip to slowly remove the culture medium from the upper layer of the liquid surface. After removing half of the volume of the old medium, new culture medium should be added using a 3 mL pipette (Bart's Pipette), with an additional 1–2 mL as needed to compensate for potential volume reduction due to evaporation in the culture system. These steps ensure the proper maintenance of the organoid culture system and support the healthy growth of the organoids.

To subculture the organoids, the mechanical digestion method is employed without the use of digestive enzymes. Following the standard protocol for partial medium change as described above, 10 mL of the old medium is discarded. Subsequently, a 1 mL regular pipette tip (reference QSP Cat: T112NXLRS-Q) is used to gently detach the organoids adhering to the container walls. Then, the same pipette tip is used to draw small, intersecting lines at the bottom of the culture container to facilitate the separation of the adherent cells in the microenvironment, after which a cell scraper is used to gently lift all the cells from the bottom. The organoids and microenvironment cell suspension are then transferred to a 15 mL tube, centrifuged at 300× *g* for 3 min, and the supernatant is discarded. Subsequently, the organoids and microenvironment cells are resuspended in preheated fresh organoid culture medium using a dedicated organoid pipette tip and seeded into a new culture container at a 5:1 split ratio for passaging.

In advance of the cryopreservation process, the organoid cryopreservation medium is prepared by combining 10 mL of the organoid cryopreservation solution (LSNO00100701; Shanghai LiSheng Biotech, China) with 0.8 mL of cryopreservation additive (LSOR00400101; Shanghai LiSheng Biotech, China). The organoids and microenvironment cells are then resuspended in the organoid cryopreservation medium using a dedicated organoid pipette tip and evenly distributed into pre-labeled cryovials, with each cryovial containing 1–1.5 mL of the cryopreservation medium. Subsequently, the cryovials are placed in a controlled-rate freezing container and stored at −80 °C in a freezer. Within one week, the cryovials can be transferred to a liquid nitrogen tank for long-term storage.

Organoids size calculation and analysis

The organoids are imaged daily, and their size is quantified using the ImageJ software. Firstly, we organize the set of photos into one file and compile them into a single image. Then, we open the file in ImageJ and use the "Polygon selections" tool to outline the outer edge of the organoids. Next, we click on "Measure" under the "Analyze" menu to calculate the area of the organoid. To assess the growth capacity of the organoid, we divide the total area by the initial area on Day 0 to obtain a relative organoid size.

Organoids drug treatments

DFSP organoids of ~ 500 μm in diameter were selected from a 10 cm dish and seeded at a density of one spheroid per well in a 24-well cell culture plate, with each well containing 1 mL of organoid culture medium. The optimal concentrations of the drugs, namely 10 μmol/L imatinib and 2.5 mmol/L metformin, were determined based on a thorough literature review and added to the respective wells containing the spheroids. Daily photographic documentation of the spheroids was performed following the addition of the drugs, and at the final time point, a detailed observation of the cellular phenotype of the spheroids was conducted.

H&E staining

Tissues and organoids were fixed in 4% paraformaldehyde (PFA) (BL539A, Biosharp) for 30 min, dehydrated with sucrose, and embedded in 7.5% gelatin. Frozen sections of 10 μm thickness were obtained using citric acid (pH 6.0). Adherent cells were fixed using 4% PFA for 20 min. For H&E staining, the sections were washed twice and stained using a H&E Stain Kit (G1120, Solarbio, China) according to the manufacturer's instructions.

Whole exon sequencing (WES)

Clinical tissues and organoids were used to isolate DNA with the Gentra Puregene Blood Kit (QIAGEN, Hilden, Germany). Each sample underwent processing with 200 ng of genomic DNA, which was fragmented into 150–200 bp fragments for library construction. The AIExome® Human Exome Panel V3 and TargetSeq One® Hyb & Wash Kit v2.0 from iGeneTech Co., Ltd, Beijing, China was employed for whole exome capture, followed by sequencing on the DNBSEQ-T7 platform with 150-bp reads. Raw reads were filtered using FastQC to eliminate low-quality reads. Subsequently, the clean reads were mapped to the reference genome GRCh37. Quality control metrics included an average read length of > 100×, accurate mapping rate of > 98%, bases capture rate of > 55%, 20× mean depth coverage rate of > 96%, duplication rate of < 25%, and accurate mapping rate of < 96%. Single nucleotide variants (SNVs) were annotated and filtered using TGex (tgex.genecards.org). This optimized approach aimed to reduce redundancy and enhance the precision of the sequencing data analysis process.

Singe cell RNA-sequencing

Skin organoids were dissociated into single cells using the Organoid Dissociation Kit (LSTO01500501; Shanghai LiSheng Biotech, China). Following the removal of erythrocytes (Solarbio R1010), cell count and viability were assessed using a fluorescence Cell Analyzer (Countstar® Rigel S2) with AO/PI reagent. Subsequently, a decision was made on whether to remove debris and dead cells using Miltenyi 130-109-398/130-090-101. The fresh cells were then washed twice in RPMI1640, re-suspended at 1 × 10^6 cells/mL in 1× phosphate buffered saline (PBS), and 0.04% bovine serum albumin was added.

For single-cell RNA-Seq library preparation, the SeekOne® Digital Droplet Single Cell' library preparation kit (SeekGene Catalog No. K00202) was utilized. Initially, the appropriate number of cells was mixed with reverse transcription reagent and added to the sample well in the SeekOne® chip. Barcoded hydrogel beads (BHBs) and partitioning oil were dispensed into corresponding wells on the chip to generate emulsion droplets. Reverse transcription was carried out at 42 °C for 90 min, followed by inactivation at 80 °C for 15 min. Subsequently, cDNA was purified, amplified in a PCR reaction, cleaned, fragmented, end repaired, A-tailed, and ligated to sequencing adaptors. Indexed PCR was then performed to amplify the DNA representing the 3' polyA part of expressing genes, which also contained Cell Barcode and Unique Molecular Index. The

indexed sequencing libraries were cleaned up with solid-phase reversible immobilization (SPRI) beads and quantified using quantitative PCR (KAPA Biosystems KK4824).

Libraries were sequenced on the Illumina Hiseq 4000 with PE-150 bp reads for subsequent analysis. Raw data from the single-cell RNA sequencing (scRNA-seq) was processed using Cell Ranger, and downstream analyses were conducted using Seurat.

Cell type identification

We utilized the publicly available dataset GSE163973, which originally identified 10 major cell types in fibrotic skin diseases. However, we encountered some cells that were unassigned or incorrectly identified. To refine the classification, we divided the "Glandular" category into "Glandular" and "T cells" due to the expression of CD3E and PTPRC (CD45) in a subset of "Glandular" cells. Additionally, we relabeled the "unknown" category as "Mast cells" based on the presence of CPA3 and PTPRC. This approach helped us construct our reference dataset[43]. Given that cell states can change during *ex vivo* culturing, harmonizing single-cell RNA sequencing (scRNA-seq) data between our organoids and the reference proved challenging. Therefore, we adopted a strategy of forced mapping of our organoid scRNA-seq data onto the reference dataset based on the Pearson correlation between the two datasets. For each cell in our organoid data, we identified the 50 most similar cells from the reference dataset. A cell was then classified based on the predominant label of these 50 cells if the same label was present in at least 40 of them; otherwise, the cell was categorized as unknown.

RNA-sequencing

mRNA was isolated from organoids using the RNA Isolation Kit (DP451, TIANGEN, China). Each group of organoids, consisting of 4–6 organoids with diameter of 2 mm, was used as input for the extraction. The concentration of RNA was measured with a Qubit4 fluorometer. Subsequently, reverse transcription was carried out using the RT Kit (KR118, TIANGEN, China), and library preparation was performed using the RNA Library Prep Kit (E7530L, NEB, USA). For bulk RNA-seq analysis, RNA expression levels were quantified using fragments per kilobase transcript mapped reads per million (FPKM), and differentially expressed genes were identified using the Morpheus online software.

Statistical analysis

The data were collected from three or more replicates, and quantitative results are expressed as mean ± standard deviation. Statistical analysis was conducted using GraphPad Prism 7.0 (GraphPad Software, USA). Student's t-test was used for multiple comparisons to assess significance. A p value less than 0.05 was considered statistically significant. The p values were calculated from a minimum of 3 independent experiments. Statistical significance is indicated as: $^{*}p < 0.05$, $^{**}p < 0.01$, and $^{***}p < 0.001$. Error bars represent the standard deviation of the mean.

Research ethics and patient consent

The collection of clinical samples followed the ethical guidelines established by Shanghai Ninth People's Hospital, with the study assigned the ethical approval No. 2017125.T321. Prior to providing samples, all participants signed informed consent forms, clearly indicating the planned utilization of their samples for future research. Their voluntary involvement and comprehension of the study's goals were crucial for maintaining ethical standards throughout this research.

Availability of data and material

The data and materials that support the findings of this study are available from the corresponding author upon reasonable request.

Declaration of conflicting interests

This work was sponsored by Shanghai Lisheng Biotech Ltd (Lisheng). The manuscript was written in a responsible and ethical manner. X.X.H. is a shareholder of Lisheng, as a founder. Y.H.S., L.Y.L., C.W., J.Z., M.J.R., J.P.L and C.H.C. are senior scientists of Lisheng. A patent on A skin fibrosarcoma like organoid model and its construction and application method has been applied (No. 2023118261310). All authors declare no competing financial interests.

X.X.H. and C.H.C. are the Editorial Board members of *Cell Organoid*. They were not involved in the journal's review of, or decisions related to, this manuscript.

Funding

The work was supported by the National Natural Science Foundation of China (Nos. 82373719, 82173662, and 32200581), Natural Science Foundation of Shanghai (No. 21ZR1436800), and Clinical Research Project of Multi-Disciplinary Team, Shanghai Ninth People's Hospital, Shanghai Jiao Tong University School of Medicine (No. 201901).

Author contributions

J.C., C.H.C., and X.X.H. conceived and designed the study. Y.H.S., L.Y.L., C.W., J.Z., and M.J.R. collected the samples, performed the experiments, and analyzed the data. J.P.L., J.C., C.H.C., and X.X.H. analyzed the data. Y.H.S., J.P.L., J.C., C.H.C., and X.X.H. wrote the manuscript. All the authors read and approved the final version of the manuscript.

Electronic Supplementary Material: Supplementary material (information of skin tumor samples and WGCNA and KEGG/GO analysis of DFSP organoids) is available in the online version of this article at https://doi.org/10.26599/CO.2024.9410001.

References

[1] Tay, S. S., Roediger, B., Tong, P. L., Tikoo, S., Weninger, W. The skin-resident immune network. *Current Dermatology Reports*, **2014**, 3(1): 13–22. https://doi.org/10.1007/s13671-013-0063-9

[2] Mestrallet, G., Rouas-Freiss, N., LeMaoult, J., Fortunel, N. O., Martin, M. T. Skin immunity and tolerance: Focus on epidermal keratinocytes expressing HLA-G. *Frontiers in Immunology*, **2021**, 12: 772516. https://doi.org/10.3389/fimmu.2021.772516

[3] Trompette, A., Ubags, N. D. Skin barrier immunology from early life to adulthood. *Mucosal Immunology*, **2023**, 16(2): 194–207. https://doi.org/10.1016/j.mucimm.2023.02.005

[4] Nestle, F. O., Di Meglio, P., Qin, J. Z., Nickoloff, B. J. Skin immune sentinels in health and disease. *Nature Reviews Immunology*, **2009**, 9(10): 679–691. https://doi.org/10.1038/nri2622

[5] Wang, T., Li, K., Xiao, S. X., Xia, Y. M. A plausible role for collectins in skin immune homeostasis. *Frontiers in Immunology*, **2021**, 12: 594858. https://doi.org/10.3389/fimmu.2021.594858
[6] Pasparakis, M., Haase, I., Nestle, F. O. Mechanisms regulating skin immunity and inflammation. *Nature Reviews Immunology*, **2014**, 14(5): 289–301. https://doi.org/10.1038/nri3646
[7] Johnson-Huang, L. M., McNutt, N. S., Krueger, J. G., Lowes, M. A. Cytokine-producing dendritic cells in the pathogenesis of inflammatory skin diseases. *Journal of Clinical Immunology*, **2009**, 29(3): 247–256. https://doi.org/10.1007/s10875-009-9278-8
[8] Turchin, I., Bourcier, M. The role of interleukins in the pathogenesis of dermatological immune-mediated diseases. *Advances in Therapy*, **2022**, 39(10): 4474–4508. https://doi.org/10.1007/s12325-022-02241-y
[9] Fetter, T., Niebel, D., Braegelmann, C., Wenzel, J. Skin-associated B cells in the pathogenesis of cutaneous autoimmune diseases—Implications for therapeutic approaches. *Cells*, **2020**, 9(12): 2627. https://doi.org/10.3390/cells9122627
[10] Xiong, D. D., Bordeaux, J. S. Incidence and survival outcomes of dermatofibrosarcoma protuberans from 2000 to 2020: A population-based retrospective cohort analysis. *Dermatologic Surgery*, **2023**, 49(12): 1096–1103. https://doi.org/10.1097/dss.0000000000004018
[11] Roh, M. R., Bae, B., Chung, K. Y. Mohs' micrographic surgery for dermatofibrosarcoma protuberans. *Clinical and Experimental Dermatology*, **2010**, 35(8): 849–852. https://doi.org/10.1111/j.1365-2230.2010.03819.x
[12] Doufekas, K., Duncan, T. J., Williamson, K. M., Varma, S., Nunns, D. Mohs micrographic surgery for dermatofibrosarcoma protuberans of the vulva. *Obstetrics and Gynecology International*, **2009**, 2009: 547672. https://doi.org/10.1155/2009/547672
[13] Zwald, F. O. Underuse of mohs micrographic surgery for the treatment of dermatofibrosarcoma protuberans. *Archives of Dermatology*, **2012**, 148(9): 1064. https://doi.org/10.1001/archdermatol.2012.2685
[14] Zeitouni, N., Cavanaugh, K., DuPont, J. Dermatofibrosarcoma protuberans: An update and review. *Current Dermatology Reports*, **2015**, 4(4): 195–204. https://doi.org/10.1007/s13671-015-0120-7
[15] Oyama, R., Kito, F., Qiao, Z. W., Sakumoto, M., Shiozawa, K., Toki, S., Yoshida, A., Kawai, A., Kondo, T. Establishment of novel patient-derived models of dermatofibrosarcoma protuberans: Two cell lines, NCC-DFSP1-C1 and NCC-DFSP2-C1. *In Vitro Cellular & Developmental Biology - Animal*, **2019**, 55(1): 62–73. https://doi.org/10.1007/s11626-018-0305-z
[16] Tang, X. Y., Wu, S., Wang, D., Chu, C., Hong, Y., Tao, M., Hu, H., Xu, M., Guo, X., Liu, Y. Human organoids in basic research and clinical applications. *Signal Transduction and Targeted Therapy*, **2022**, 7: 168. https://doi.org/10.1038/s41392-022-01024-9
[17] Xu, H. X., Jiao, D. C., Liu, A. G., Wu, K. M. Tumor organoids: Applications in cancer modeling and potentials in precision medicine. *Journal of Hematology & Oncology*, **2022**, 15(1): 58. https://doi.org/10.1186/s13045-022-01278-4
[18] Zhou, Z., Cong, L., Cong, X. Patient-derived organoids in precision medicine: Drug screening, organoid-on-a-chip and living organoid biobank. *Frontiers in Oncology*, **2021**, 11: 762184. https://doi.org/10.3389/fonc.2021.762184
[19] Forsythe, S. D., Sivakumar, H., Erali, R. A., Wajih, N., Li, W. C., Shen, P., Levine, E. A., Miller, K. E., Skardal, A., Votanopoulos, K. I. Patient-specific sarcoma organoids for personalized translational research: Unification of the operating room with rare cancer research and clinical implications. *Annals of Surgical Oncology*, **2022**, 29(12): 7354–7367. https://doi.org/10.1245/s10434-022-12086-y
[20] Lei, M. X., Schumacher, L. J., Lai, Y. C., Juan, W. T., Yeh, C. Y., Wu, P., Jiang, T. X., Baker, R. E., Widelitz, R. B., Yang, L. et al. Self-organization process in newborn skin organoid formation inspires strategy to restore hair regeneration of adult cells. *Proceedings of the National Academy of Sciences of the United States of America*, **2017**, 114(34): E7101–E7110. https://doi.org/10.1073/pnas.1700475114
[21] Hong, Z. X., Zhu, S. T., Li, H., Luo, J. Z., Yang, Y., An, Y., Wang, X., Wang, K. Bioengineered skin organoids: From development to applications. *Military Medical Research*, **2023**, 10(1): 40. https://doi.org/10.1186/s40779-023-00475-7
[22] Navarrete-Dechent, C., Mori, S., Barker, C. A., Dickson, M. A., Nehal, K. S. Imatinib treatment for locally advanced or metastatic dermatofibrosarcoma protuberans: A systematic review. *JAMA Dermatology*, **2019**, 155(3): 361–369. https://doi.org/10.1001/jamadermatol.2018.4940
[23] Johnson-Jahangir, H., Sherman, W., Ratner, D. Using imatinib as neoadjuvant therapy in dermatofibrosarcoma protuberans: Potential pluses and minuses. *Journal of the National Comprehensive Cancer Network*, **2010**, 8(8): 881–885. https://doi.org/10.6004/jnccn.2010.0065
[24] Rutkowski, P., Wozniak, A., Switaj, T. Advances in molecular characterization and targeted therapy in dermatofibrosarcoma protuberans. *Sarcoma*, **2011**, 2011: 959132. https://doi.org/10.1155/2011/959132
[25] Peng, C., Jian, X. X., Xie, Y., Li, L. F., Ouyang, J., Tang, L., Zhang, X., Su, J., Zhao, S., Liu, H. et al. Genomic alterations of dermatofibrosarcoma protuberans revealed by whole-genome sequencing. *British Journal of Dermatology*, **2022**, 186(6): 997–1009. https://doi.org/10.1111/bjd.20976
[26] Deng, C. C., Hu, Y. F., Zhu, D. H., Cheng, Q., Gu, J. J., Feng, Q. L., Zhang, L. X., Xu, Y. P., Wang, D., Rong, Z. L. et al. Single-cell RNA-seq reveals fibroblast heterogeneity and increased mesenchymal fibroblasts in human fibrotic skin diseases. *Nature Communications*, **2021**, 12: 3709. https://doi.org/10.1038/s41467-021-24110-y
[27] Ge, L. L., Wang, Z. C., Wei, C. J., Huang, J. X., Liu, J., Gu, Y. H., Wang, W., Li, Q. F. Unraveling intratumoral complexity in metastatic dermatofibrosarcoma protuberans through single-cell RNA sequencing analysis. *Cancer Immunology, Immunotherapy*, **2023**, 72(12): 4415–4429. https://doi.org/10.1007/s00262-023-03577-2
[28] Kemper, K., Krijgsman, O., Cornelissen-Steijger, P., Shahrabi, A., Weeber, F., Song, J. Y., Kuilman, T., Vis, D. J., Wessels, L. F., Voest, E. E. et al. Intra- and inter-tumor heterogeneity in a vemurafenib-resistant melanoma patient and derived xenografts. *EMBO Molecular Medicine*, **2015**, 7(9): 1104–1118. https://doi.org/10.15252/emmm.201404914
[29] Kerkour, T., Zhou, C., Hollestein, L., Mooyaart, A. Genetic concordance in primary cutaneous melanoma and matched metastasis: A systematic review and meta-analysis. *International Journal of Molecular Sciences*, **2023**, 24(22): 16281. https://doi.org/10.3390/ijms242216281
[30] Skuli, S. J., Alomari, S., Gaitsch, H., Bakayoko, A., Skuli, N., Tyler, B. Metformin and cancer, an ambiguanidous relationship. *Phamaceuticals*, **2022**, 15(5): 626. https://doi.org/10.3390/ph15050626
[31] Hua, Y., Zheng, Y., Yao, Y. R., Jia, R. B., Ge, S. F., Zhuang, A. Metformin and cancer hallmarks: Shedding new lights on therapeutic repurposing. *Journal of Translational Medicine*, **2023**, 21(1): 403. https://doi.org/10.1186/s12967-023-04263-8
[32] Jacob, F., Salinas, R. D., Zhang, D. Y., Nguyen, P. T. T., Schnoll, J. G., Wong, S. Z. H., Thokala, R., Sheikh, S., Saxena, D., Prokop, S. et al. A patient-derived glioblastoma organoid model and biobank recapitulates inter- and intra-tumoral heterogeneity. *Cell*, **2020**, 180(1): 188–204.e22. https://doi.org/10.1016/j.cell.2019.11.036
[33] LeBlanc, V. G., Trinh, D. L., Aslanpour, S., Hughes, M., Livingstone, D., Jin, D., Ahn, B. Y., Blough, M. D., Cairncross, J. G., Chan, J. A. et al. Single-cell landscapes of primary glioblastomas and matched explants and cell lines show variable retention of inter- and intratumor heterogeneity. *Cancer Cell*, **2022**, 40(4): 379–392.e9.

https://doi.org/10.1016/j.ccell.2022.02.016

[34] Choe, M. S., Kim, S. J., Oh, S. T., Bae, C. M., Choi, W. Y., Baek, K. M., Kim, J. S., Lee, M. Y. A simple method to improve the quality and yield of human pluripotent stem cell-derived cerebral organoids. *Heliyon*, **2021**, 7(6): e07350. https://doi.org/10.1016/j.heliyon.2021.e07350

[35] Hu, Y. W., Sui, X. Z., Song, F., Li, Y. Q., Li, K. Y., Chen, Z. Y., Yang, F., Chen, X. Y., Zhang, Y. H., Wang, X. N. et al. Lung cancer organoids analyzed on microwell arrays predict drug responses of patients within a week. *Nature Communications*, **2021**, 12: 2581. https://doi.org/10.1038/s41467-021-22676-1

[36] Shankaran, A., Prasad, K., Chaudhari, S., Brand, A., Satyamoorthy, K. Advances in development and application of human organoids. *3 Biotech*, **2021**, 11(6): 257. https://doi.org/10.1007/s13205-021-02815-7

[37] Calà, G., Sina, B., De Coppi, P., Giobbe, G. G., Gerli, M. F. M. Primary human organoids models: Current progress and key milestones. *Frontiers in Bioengineering and Biotechnology*, **2023**, 11: 1058970. https://doi.org/10.3389/fbioe.2023.1058970

[38] Suarez-Martinez, E., Suazo-Sanchez, I., Celis-Romero, M., Carnero, A. 3D and organoid culture in research: Physiology, hereditary genetic diseases and cancer. *Cell & Bioscience*, **2022**, 12(1): 39. https://doi.org/10.1186/s13578-022-00775-w

[39] Cruz-Gil, S., Sánchez-Martínez, R., Wagner-Reguero, S., Stange, D., Schölch, S., Pape, K., Ramírez de Molina, A. A more physiological approach to lipid metabolism alterations in cancer: CRC-like organoids assessment. *PLoS One*, **2019**, 14(7): e0219944. https://doi.org/10.1371/journal.pone.0219944

[40] Finisguerra, V., Dvorakova, T., Formenti, M., Van Meerbeeck, P., Mignion, L., Gallez, B., Van den Eynde, B. J. Metformin improves cancer immunotherapy by directly rescuing tumor-infiltrating CD8 T lymphocytes from hypoxia-induced immunosuppression. *Journal for ImmunoTherapy of Cancer*, **2023**, 11(5): e005719. https://doi.org/10.1136/jitc-2022-005719

[41] Conza, D., Mirra, P., Fiory, F., Insabato, L., Nicolò, A., Beguinot, F., Ulianich, L. Metformin: A new inhibitor of the Wnt signaling pathway in cancer. *Cells*, **2023**, 12(17): 2182. https://doi.org/10.3390/cells12172182

[42] Mamedov, M. R., Vedova, S., Freimer, J. W., Das Sahu, A., Ramesh, A., Arce, M. M., Meringa, A. D., Ota, M., Chen, P. A., Hanspers, K. et al. CRISPR screens decode cancer cell pathways that trigger γδ T cell detection. *Nature*, **2023**, 621(7977): 188–195. https://doi.org/10.1038/s41586-023-06482-x

[43] Menden, K., Marouf, M., Oller, S., Dalmia, A., Magruder, D. S., Kloiber, K., Heutink, P., Bonn, S. Deep learning–based cell composition analysis from tissue expression profiles. *Science Advances*, **2020**, 6(30): eaba2619. https://doi.org/10.1126/sciadv.aba2619